MODELLING MICROMECHANISMS AND STATISTICAL FEATURES OF DUCTILE FRACTURE

A. PINEAU*

Ductile rupture involves three successive stages : cavity nucleation, void growth and coalescence, which are briefly reviewed. Then recent developments to model ductile rupture, based on the mechanics of porous materials are underlined, as well as the importance of the inhomogeneity in cavity distribution. These models are used to predict the variation of ductility with stress triaxiality observed in steels, Al alloys and a cast duplex stainless steel. In this material a model is introduced to predict also the scatter and the size effect observed on notched tensile specimens. Simple approaches are also presented to model the fracture toughness of these materials.In particular a statistical model based on a Monté-Carlo type simulation is presented to calculate the fracture toughness of a duplex stainless steel in which continuous cavity nucleation from cleavage cracks formed in the ferrite phase plays a predominant role.

INTRODUCTION

It is well known that, in most structural materials, ductile rupture involves three stages. The first stage is associated with the nucleation of cavities which take place from particles, such as inclusions, or occasionally from one of the phases present in multiphase materials. It is clear that, if cavity nucleation could be delayed, large improvements in ductility and fracture toughness could be achieved. It is therefore important to investigate the metallurgical factors and the mechanical variables controlling this first stage of ductile rupture. Then the growth of cavities initiated from the above sites takes place, followed by cavity coalescence. A large research effort has been made over the past decade to model the last stage of ductile fracture in order to derive fracture criteria which can be incorporated in the analysis of crack tip stress-strain field to predict the fracture toughness of structural materials. These models are largely based on the mechanics of porous materials. In many cases it is assumed that the cavities are homogeneously distributed, which is far from the actual situation met in structural materials. This is the reason why in the present paper a large attention is paid to the effect of the non-uniform distribution of cavities on the ductility and the fracture toughness.

The paper is divided into two main parts. The micromechanisms of ductile fracture and the mechanics of porous materials are firstly reviewed. In this part, the emphasis is laid upon the importance of the inhomogeneity of plastic

*Centre des Matériaux Ecole des Mines B.P.87 - 91003 EVRY Cédex (France)
URA CNRS 866.

strain between the matrix and the second phase particles, and upon the effect of the inhomogeneity of cavity distribution. In particular it is shown that it is possible to model the ductility of multiphase materials, such as duplex stainless steels, in which the statistical nature of continuous cavity nucleation plays a predominant role. This first part deals with the mechanical behaviour of elementary volume elements while, in the second part, models used for predicting the fracture toughness of structural materials are briefly reviewed.

DUCTILE RUPTURE

Cavity nucleation

When nucleation sites are associated with large ($\geq$ 1 μm) and widely spaced particles, discontinuous nucleation can be described in terms of continuum mechanics. A nucleation model based on the existence of a critical stress, σ_d, was thus proposed by Argon et al [1] as :

$$\sigma_d = \sigma_{eq} + \sigma_m \tag{1}$$

where σ_{eq} is the local equivalent von Mises stress, while σ_m is the hydrostatic stress. In Eq. 1, the inhomogeneity in plastic deformation between the matrix and the inclusions does not appear explicitly. This appears more clearly in the expression proposed by Beremin [2] to account for cavity nucleation from MnS inclusions in low alloy steels. This expression which was derived from the application of inclusion theory developed by Eshelby [3] can be written as :

$$\sigma_d = \Sigma_1 + k\,(\sigma_{eq} - \sigma_o) \tag{2}$$

where Σ_1 is the maximum principal stress, σ_o the yield strength, and k is a function of particle shape.

These expressions can only be applied to model discontinuous nucleation, but it is usually observed that void nucleation occurs continuously over a wide range of strains, sometimes after only a critical strain has been reached. Moreover large inclusions are often observed to be preferential sites. This may arise for several reasons [4] : (i) Large inclusions have a greater probability of containing volume or surface flaws; (ii) Large particles have more difficulty of relaxing large stress concentrations; (iii) Interactions effects between inclusions of larger than average size and spacing. This results in an increasing number of cavity sites with plastic strain.

Whether continuous nucleation is a strain-or stress-controlled phenomenom is still widely discussed. Kwon and Asaro [4] concluded that an interfacial stress-controlled nucleation criterion was more realistic than a strain-controlled criterion to characterize the nucleation behaviour of spheroidized steels. On the other hand, the results obtained on Al alloys by Walsh et al [5] and on a cast duplex stainless steel by Pineau and Joly [6] and by Joly et al [7] indicate that cavity nucleation is essentially strain-controlled. The latter material (CF8M steel) contains about 25% of ferrite phase embedded in a large grain ($\sim$ 1 mm) and ductile austenite matrix. The ferrite phase is embrittled after prolonged aging for 700 hours at 450°C. This

results in a material with a low Charpy toughness of about 3 daJ/cm^2 at R.T. Interrupted tensile tests show that cleavage cracks are nucleated within ferrite islands (Fig.1a), and then grow as cavities which are preferentially located in a number of clusters (Fig.1b). It was shown that these clusters of damaged material were preferentially located within the austenite grains oriented for single slip [7]. This strong inhomogeneity in cavity nucleation is likely due to the high deformation incompatibility between both phases which have different crystallographic structure and different hardness. The incompatibility is more pronounced when austenite is deformed in single slip [8]. Measurements of the number of cracks per unit area showed that the density of cracks increases in these grains, and that new clusters were formed when the plastic strain was increased. In this material the component of the volume fraction of porosity associated with the nucleation could be expressed as :

$$df_n = A_n \, d\varepsilon_{eq} \tag{3}$$

where $d\varepsilon_{eq}$ is the increment of the equivalent plastic strain, while A_n is the nucleation rate, which is assumed to be constant but to be distributed from grain to grain, as indicated above.

Cavity growth

Substantial progress in the understanding of void growth has been made through the theoretical models by Berg [9], Mc Clintock [10], and Rice and Tracey [11]. These models are based on a number of simplifying assumptions which do not necessarily apply to real materials. In particular, they assume that there is no interaction effect between neighbouring cavities. In the Rice and Tracey model, the cavity growth rate at large stress triaxiality is given by :

$$D = dR/R \, d\varepsilon_{eq} = df/3f(1-f) \, d\varepsilon_{eq} = 0.283 \exp(3\sigma_m/2\sigma_{eq}) \tag{4}$$

where R is the cavity size, f, the volume fraction and σ_m, the hydrostatic stress. In the literature there are relatively few experimental verifications of this expression. However recently a comparison between the results of numerical calculations and experiments was made by Worswick and Pick [12], who showed that a number of experimental results [13-15] were in good agreement with Eq.4, except for the preexponential term which was found to be larger than 0.283. This difference may arise from several reasons. The first reason lies in the fact that a recent analytical work by Huang et al [16] indicates that the widely used high triaxiality approximation (Eq.4) underestimates the cavity dilatation rate by more than 50% at all levels of stress triaxiality above $\sigma_m/\sigma_{eq} = 1$. Another reason might be due to the fact that, as a rule, structural materials contain a second population of cavities nucleated from particles, such as carbides in steels or strengthening precipitates in Al alloys. A limited number of metallographic observations similar to those reported by Marini et al [15] tend to show that the growth of large cavities initiated from inclusions can be accelerated by the presence of smaller voids initiated from carbides and located in their vicinity. Recently the growth of cavities in a two population material has been treated theoretically by Leblond and Perrin [17]. In their model the matrix is assumed to have a spherical shape with an initial volume

fraction f_1 and is submitted to a hydrostatic stress Σ_m, as shown in Fig.2a. A damaged zone of radius, a, with a different volume fraction, f_2, is located at the center of the sphere of radius, b. The results of the analytical model are shown in Fig.2b where f_1 (∞) corresponds to the condition b --> ∞. In all cases, it is noticed that the local void growth rate in the matrix at r = a is larger than at infinity (r --> ∞). In particular, when f_2/f_1 --> ∞, ie in the case of a central cavity, the local void growth rate is twice that corresponding at infinity. Furthermore, this figure shows that the void growth rate associated with the central inhomogeneity, measured by the ratio $\dot{f}_2 / f_2(1-f_2) / \dot{f}_1(\infty) / f_1(1-f_1)$ is larger than that of the matrix when $f_2/f_1 > 1$.

Cavity coalescence and criteria for ductile rupture

The last stage of ductile rupture requires a large research effort and a large number of approximations to keep the problem tractable. This section is divided into three parts. It is firstly shown that the criterion for ductile rupture based on critical void growth, initially introduced by McClintock [18] and then used by a number of authors, can still be extremely useful. Then, the developments achieved by the introduction of the mechanics of porous materials are presented. The limitations of these developments due to the fact that the inhomogeneity in cavity distribution is not properly taken into account are underlined. Finally, it is shown how this important feature of cavitating materials can be incorporated either to predict the anisotropy of ductile rupture in Al alloys or to model the scatter and the size effects observed in the ductile rupture of cast duplex CF8M stainless steel.

Critical void growth at fracture

When the strain for cavity nucleation represents only a small fraction of the ductility, the simplest criterion is obtained by integrating Eq.4 and by assuming that fracture takes place for a critical porosity [18]. For a stress history during which the stress triaxiality is kept constant, this leads to :

$$\mathrm{Ln}(R / R_o)_c = 1/3\ \mathrm{Ln}(f / f_o)_c = 0.283\ \varepsilon_R\ \exp(3\sigma_m / 2\sigma_{eq}) \qquad (5)$$

In a number of cases, including C-Mn-Ni-Mo steels containing various amounts of MnS inclusions (Pineau [19]) and, more recently 7XXX Al alloys containing different amounts of Fe and Si-rich particles (Achon and Pineau [20]), it was shown that Eq.5 was relatively well satisfied. Examples illustrating the situation observed in two high strength Al alloys containing two widely different volume fractions of Fe-rich particles are shown in Fig.3. In these materials, tensile tests were carried out on axisymmetrically notched specimens cut along the three main directions of thick plates. The geometry of these specimens which is similar to that used in other studies, (see eg.[6,19]) was chosen in such manner to produce different stress triaxialities. In all cases, similarly to C-Mn-Ni-Mo steels, it is observed that, within a first approximation, $\mathrm{Ln}\varepsilon_R$ is proportionnal to σ_m/σ_{eq} with a slope of - 3/2, as predicted by Eq.5. In Al alloys, the calculated critical void growth, $(R/R_O)_c$, is found to be extremely small, especially in the short-transverse direction (typically 1.05 to 1.15). These values are still smaller than those calculated in steels [19].

Here it should also be added that, in many situations, cavity nucleation cannot be neglected. This should produce different variations of ductility with stress triaxiality. The situation corresponding to the CF8M steel mentioned earlier is a good example to illustrate this specific point (see [6,8] and Pineau [21]. In this material, in adding the nucleation component (Eq.3) to the growth term (Eq.4), it can easily be shown that, if it is assumed that ductile fracture occurs for a critical volume fraction of cavities, f_c, then the variation of ductility with stress triaxiality can simply be expressed as :

$$\varepsilon_R = 1/K.Ln\left[1+K(f/A_n)_c\right] \tag{6}$$

where $K = 3 \times 0.283 \exp(3\sigma_m/2\sigma_{eq})$. This expression is plotted in Fig.4 for various values of $(f/A_n)_c$. This figure clearly shows that, as expected, for large values of A_n, the ductility is no longer strongly dependent on σ_m/σ_{eq}. In Fig. 4, we have also reported the experimental results obtained on CF8M steel. These results show that, in this material in which cavity nucleation plays a predominant role, as indicated earlier, the ductility is only slightly dependent on stress triaxiality, which was not the situation observed in ferritic steels [2,6,19,21] or in Al alloys [20].

Mechanics of porous materials

Many studies have been devoted, over the past decade, to model the softening effect produced by growing cavities and void coalescence, using the mechanics of porous materials. In these models the plastic flow potential is dependent on cavity volume fraction. It is beyond this paper to review all the existing theories but, instead, to show how these theories can be used to model ductile rupture. Here we refer only to the Gurson-Tvergaard (GT) and the Rousselier models.

In the GT potential, the yield criterion is written as (Tvergaard [22]) :

$$\sigma_{eq}^2/Y^2 + 2q_1 f \cosh(3q_2\sigma_m/2Y) - 1 - q_3 f^2 = 0 \tag{7}$$

where Y is the flow stress of the undamaged matrix. It was shown [22] that $q_1 \sim 1.5$, $q_2 \sim 1$ and $q_3 = q_1^2$. More recently, using a self consistent scheme, it was shown by Perrin and Leblond that $q_1 = 4/e = 1.47$ [23]. For small volume fractions, Eq.7 can be simplified as :

$$\sigma_{eq} = \sqrt{(3/2)s_{ij}s_{ij}} = Y\left[1-0.50f \exp(3\sigma_m/2Y)\right] \tag{8}$$

where the softening effect due to the presence of cavities appears clearly to be more pronounced at large stress triaxiality, as expected. The associated increment in cavity volume fraction is given by :

$$d\varepsilon_{ii} = df/(1-f) = 0.75\, f \exp(3\sigma_m/2Y).d\varepsilon_{eq} \tag{9}$$

which is very similar to Eq.4.

The application of the GT potential was reviewed by Needleman [24]. In the simulation of ductile fracture of a material in which the cavities are assumed to be homogeneously distributed, it was shown that this model largely overestimated the observed ductility of structural materials. An accelerating function f* was introduced by Tvergaard and Needleman [25] to simulate the effect of void coalescence. Initially f* = f calculated from Eq.9 but, at some critical volume fraction, f_c, f* is written as $f^* = f_c + \delta (f-f_c)$ where δ is an accelerating factor. This model therefore bears a strong resemblance with the $(R/R_0)_c$ criterion. In both cases, they can be considered to be "black boxes" in the absence of a proper account of cavity distribution. The effect of a non-uniform distribution of porosity on failure in a porous material was analyzed numerically by Becker [26] using the same modification of the GT potential. This author showed that a failure criterion based on a critical void volume fraction that is only weakly dependent on stress triaxiality was appropriate. This reinforces the soundness of the $(R/R_0)_c$ criterion. Here it should also be added that the GT potential has also been used to model the toughness of Charpy V specimens [27,28]).

The yield function proposed by Rousselier [29,30] can be written as :

$$\sigma_{eq} / (1-f)Y = 1 - [DB(\beta) / Y] \exp [\sigma_m / (1-f)\sigma_1] \qquad (10)$$

with :

$$d\beta = df / f(1-f) = D \exp [\sigma_m / (1-f)\sigma_1] \, d\varepsilon_{eq} \qquad (11)$$

and

$$B(\beta) = \sigma_1 f_0 \exp \beta / (1 - f_0 \exp \beta) \qquad (12)$$

This function bears also a strong resemblance with the GT potential, provided that it is assumed that D = 3 x 0.25 and σ_1 = 2Y/3. Rousselier implemented his criterion in a F.E.M. code to simulate the failure of notched bars (see also [6]) but, similarly to the other models (f_c in the GT potential), it was necessary to introduce another parameter, here the mesh size, ℓ_c, to simulate plastic flow localization and ductile fracture. In the following one way of avoiding the use of these fitting parameters, such a f_c or ℓ_c, is introduced by using the distribution of cavities.

Anisotropy, scatter and size effects in ductile rupture

Mudry [31] has also used the GT potential to model the ductile fracture of C-Mn-Ni-Mo steels, but without introducing the accelerating effect in f used by Tvergaard and Needleman [25]. The basis of the model is schematically shown in Fig.5 where the undamaged stress-strain curve of the matrix is compared to those corresponding to different values of the initial volume fraction of cavities, f_0. Fracture of a component, such as a notched specimen, is assumed to take place if there is a non-vanishing probability of finding a volume element for which the local volume fraction is such that the associated stress-strain curve reaches a maximum. The macroscopic ductility is then calculated, as indicated in Fig.5, assuming that the elementary volume elements are assembled either in series or in parallel.

More recently this approach was used to predict the ductility of axisymmetrically notched specimens of two high strength Al alloys, containing widely different values of inclusions [20]. In these materials, the Fe,Si-rich particles are strongly inhomogeneously distributed as a consequence of hot rolling deformation. Quantitative metallography was used to draw the Voronoï cells associated with the inclusions. Then an original procedure based on the distance between neighbours [8,32] was used to isolate the clusters of inclusions which present a local density much higher than in their neighbourhood (see eg. Fig.6 where two different section planes are shown). An effective volume fraction, f_{eff}, was then calculated from these observations. f_{eff} was defined as the volume fraction of spherical inclusions which have the same surface as the area of the clusters projected on the presumed fracture surface. This volume fraction which is significantly larger than the mean volume fraction was then compared to that inferred from the approach presented earlier (f_{pred}). Fig.7 shows a good agreement between both values of f determined in the three main directions of the rolled plates.

A similar approach was adopted to model the ductility of notched specimens of CF8M steel [8,32]. In this material it was shown earlier that the damaged zones were grouped into clusters (Fig.1). This time, the size and the mean distance of the clusters is such that they cannot be considered to be homogeneously distributed. A statistical analysis, based on a Monte-Carlo simulation, of the fracture of axisymmetrically notched specimens was carried out, using finite element calculations. The number of damaged grains, their position and their nucleation rate A_n (Eq.3) were regarded as random. The details of the calculations are given elsewhere [32]. Fig.8 shows a good agreement between the experimental and the simulated data. The large scatter observed both experimentally and numerically is attributed to the small number of austenite grains unfavorably oriented (single slip) with respect to the specimen size, combined with the large scatter of A_n in these grains. The decrease of the scatter predicted by the model for smooth specimens could be related to an important size effect. However a specific study showed that one reason for the higher experimental scatter observed in these specimens was due to the fact that the effective volume of smooth specimens must be reduced because of the existence of local necking which was not taken into account in the model. Further tests on notched specimens with the same geometry but with different dimensions were carried out to investigate the size effects. The results are given in Fig.9 where it is observed that the model predicts correctly the decrease of the ductility observed when the specimen size is increased.

FRACTURE TOUGHNESS

At the crack tip, as in many models based on local criteria, it is necessary to introduce a characteristic distance, λ, the famous "process zone". The strains and the stresses are averaged over this distance. In F.E.M. calculations this size is used for the first element located at the crack tip. The choice of this size is not too critical for a stress-controlled failure mode due to crack tip blunting effect, but it is much more critical for a strain-controlled failure mode, ie typically in ductile rupture. Theoretically the introduction of constitutive equations in which a coupling effect with damage is introduced, such as the flow potentials introduced earlier should contribute in solving this difficult problem. However, as indicated

above, in these models, there are still a number of variables which must still be considered to be adjustable parameters.

In spite of these difficulties it should be kept in mind that there exist in the literature a number of models based on this averaging procedure which are extremely useful (For a review, see eg.[21]. In materials for which cavity nucleation can be neglected, a model based on the calculated average void growth was shown to be satisfactory. This was applied to the prediction of the fracture toughness of C-Mn-Ni-Mo steels in which cavities are easily nucleated from MnS inclusions. For small scale yielding (SSY) conditions, it was shown [34] that there exists a relationship between J_{IC} and Ln $(R/R_O)_c$:

$$J_{IC} = \alpha \lambda \sigma_O \text{ Ln } (R/R_O)_c \qquad (12)$$

where λ is the mean distance between inclusions in a plane perpendicular to the crack front and α is a numerical factor. For large scale yielding (LSY) conditions this model was used to show that the values of J_{IC} were not intrinsic, but dependent on specimen geometry. In particular, the values of J_{IC} are predicted to be larger in CP type specimens which are subject to tensile loads than in CT type specimens which are essentially submitted to bending stresses. The prediction has now received a number of experimental evidences (see eg. [35,36]. Similar approaches have to be developed to model the fracture toughness of materials in which cavity nucleation occurs continuously and cannot be neglected. A good example is provided by multiphase materials similar to the duplex stainless steel described earlier.

For this material in which large inhomogeneities in the spatial distribution of damage zones is observed (Fig.1), a model based on a Monte-Carlo simulation similar to that used for notched specimens was developed. The details are given elsewhere [33]. The results of the numerical simulations are shown in Fig.10 where the distribution of $J_{O.2}$ results as predicted from the model for 18 mm thick specimens is compared to a number of experimental results [8,37]. A large set of experimental data is needed to compare the results of the model, on a statistical basis, especially for the lower tail of the distribution. However this model is in broad agreement with the experiments, which is all the more encouraging as it is essentially based on microstructural parameters. It can also be added that this model was also used to predict the size effect, as earlier in notched specimens. CT specimens with the same in-plane dimensions but with different thickness were modelled. The results are given in Fig.11. This figure shows the median of $J_{O.2}$ (50 th percentile) which is very close to the average, the 16th and the 3th percentiles calculated from 100 simulations. Unlike the case of notched specimens (Fig.9), there is almost no effect on the average. This results from the fact that, in tensile notched specimens, fracture is controlled by the failure of the most damaged grains, and it is well known that the statistics of extreme cases depends on the sample size. On the other hand, in the model, for CT specimens, crack growth is the sum of the growth contribution for all the damaged grains and results therefore from an averaging process. However when extreme cases are considered we can notice, for example, that the 3th percentile increases with specimen thickness. The probability of finding an extremely low value for the fracture toughness is much lower for a thick specimen than for a small one. This expected behaviour may have strong practical implications both for mechanical testing and for the use of conservative values in the assessment of the structural integrity of components.

CONCLUSIONS

The micromechanisms and the mechanics of the three stages for ductile rupture have been briefly described. In a number of materials, such as ferritic steels or Al alloys, it is shown that cavity nucleation occurs at a critical strain which may be a function of stress triaxiality, while in other materials, such as duplex stainless steels, void nucleation must be modelled as a continuous process. In all cases, statistical aspects such as the inhomogeneity in the cavity distribution play a key role. These statistical features account for the scatter in the results and, in some cases, for the size effect observed when testing specimens of different sizes. The mechanics of porous materials is a very promising tool to model the softening effect associated with cavitation, provided that the statistical distribution of cavities is taken into account. When the deviation from a homogeneous distribution occurs over large distances, it may be necessary to use statistical models, based on a Monte-Carlo simulation, as shown in a duplex stainless steel.

Simple expressions between the fracture toughness and local criteria, such as critical void growth, have been established for small scale yielding conditions. Similar expressions do not exist for large scale yielding conditions when the toughness cannot be described by a single loading parameter. The potential of a model incorporating the statistical aspects of ductile damage encountered in a duplex stainless steel is highlighted. This model was used to predict not only the scatter but also the size effects observed in this material.

REFERENCES

(1) Argon, A.S., Im, J., and Safoglu, R., Met. Trans. Vol.6A, 1975, pp.825-937.

(2) Beremin, F.M., Met. Trans., Vol.12A, 1981, pp.723-731.

(3) Eshelby, Proc.R., Soc., Vol.A 241, 1957, p.376.

(4) Kwon, D., and Asaro, R.J., Met. Trans., Vol.21A, 1990, pp.117-134.

(5) Walsh, J.A., Jata, K.V., and Starke, E.A., Acta Metall., Vol.37, 1989, pp.2861-2871.

(6) Pineau, A., and Joly P., Local versus global approaches to elastic-plastic fracture mechanics. Application to ferritic steels and a cast duplex stainless steel. ESIS/EGF9, 1991, pp.381-414.

(7) Joly, P., Cozar, R., and Pineau A., Scripta Metall., Vol.24, 1990, pp.2235-2240.

(8) Joly, P., Etude de la rupture d'aciers inoxydables austéno-ferritiques moulés fragilisés par vieillissement à 400°C. Thesis Ecole des Mines, May 21, 1992.

(9) Berg, C.A., Proc. 4th U.S. National Congress of Applied Mechanics, Univ. of California, 1962, June 18-21.

(10) Mc Clintock, F.A., J. App. Mech., Vol. 35, 1968, pp.363-371.

(11) Rice, J.R. and Tracey, D.M., J. Mech. Phys. Solids, Vol.17, 1969, pp.201-207.

(12) Worswick, M.J. and Pick, R.J., J. Mech. Phys. Solids, Vol.38, 1990, pp.610-625.

(13) Bourcier, R.J., Koss, D.A., Smelser, R.E. and Richmond, O., Acta Metall., Vol.34, 1986, pp.2443-2452.

(14) Barnby, J.T., Shi, Y.W. and Nadkani, A.S., Int. J. Fracture, Vol.25, 1984, pp.273-283.

(15) Marini, B., Mudry, F. and Pineau, A., Eng. Fracture Mechanics, Vol.22, 1985, pp.989-996.

(16) Huang, Y., Hutchinson, J.W. and Tvergaard, V., J. Mech. Phys. Solids,Vol.39, 1991, pp.223-241.

(17) Perrin, G. Contribution à l'étude théorique et numérique de la rupture ductile des métaux. Thesis, Ecole Polytechnique, July 8, 1992.

(18) Mc Clintock, F.A., Plasticity aspects of fracture, in Liebowitz, H. Ed. Fracture, Vol.3, 1971, pp.47-225.

(19) Pineau, A., Review of fracture micromechanisms and a local approach to predicting crack resistance in low strength steels, in François et al., Ed. Advances in Fracture Research, ICF5, Cannes, 1981, pp.553-577.

(20) Achon, Ph. and Pineau, A. Unpublished research.

(21) Pineau, A., Global and local approaches of fracture - Transferability of laboratory test results to components, in Argon, A.S., Ed. Topics in fracture and fatigue, Springer Verlag, 1992, pp.196-234.

(22) Tvergaard, V., Int. J. Solids Struct., Vol.18, 1982, p.659.

(23) Perrin, G. and Leblond, J.B., Int. J. Plasticity, Vol.6, 1990, pp.677-699.

(24) Needleman, A., Theoretical and Applied Mechanics, Germain, P. et al. Ed. Elsevier Science Publishers. IUTAM, 1989, pp.217-240.

(25) Tvergaard, V. and Needleman, A., Acta Met., Vol.32, 1984, pp.157-169.

(26) Becker, J., J. Mech. Phys. Solids, Vol.35, 1987, pp.577-599.

(27) Tvergaard, V. and Needleman, A., J. Mech. Phys. Solids, Vol.34, 1986, p.213-241.

(28) Böhme, W., Sun, D.Z., Schmitt, W. and Höning, A., AMD, Vol.137,. Advances in local fracture/damage models for the analysis of engineering problems, Giovanola, J.H. and Rosakis, A.J. Ed., ASME, 1992, pp.203-216.

(29) Rousselier, G., Contribution à l'étude de la rupture des métaux dans le domaine de l'élasto-plasticité, Thesis, Ecole Polytechnique, 1979.

(30) Rousselier, G., Nucl. Eng. Design., Vol.105, 1987, pp.97-111.

(31) Mudry, F., Etude de la rupture ductile et de la rupture par clivage d'aciers faiblement alliés. Thesis, 1982.

(32) Joly, P., Meyzaud, Y. and Pineau, A., AMD , Vol.137, Advances in local fracture/damage models for the analysis of engineering problems, Giovanola, J.H. and Rosakis, A.J., Ed., ASME, 1992, pp.151-180.

(33) Joly, P., Pineau, A. and Meyzaud, Y., in Mecamat 93, Int. seminar on micromechanics of materials, Eyrolles, 1993, pp.210-221.

(34) Mudry, F., Di Rienzo, F. and Pineau, A., ASTM STP 995, 1988, pp.24-39.

(35) Garwood, S.J., Int. J. Pressure Vessels Piping, Vol.10, 1982, pp.297-319.

(36) Marandet, B., Phelippeau, G., De Roo, G. and Rousselier, G., ASTM STP 833, 1984, pp.606-621.

(37) Bonnet, S., Bourgoin, J., Champredonde, J. and Guttman, D., Materials Science and Technology, Vol.6, 1990, pp.221-229.

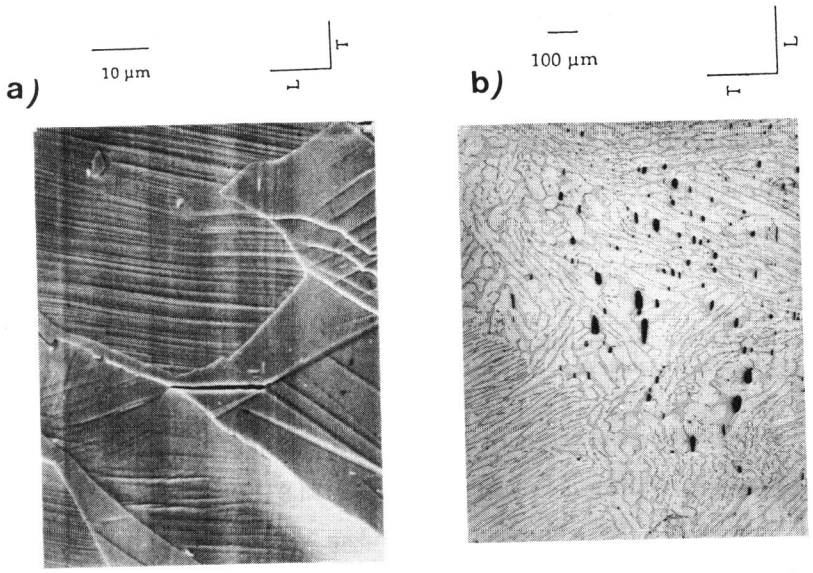

Figure 1 CF8M Steel. a) Cleavage crack formed at the intersection of two mechanical twins; b) Cavities initiated from cleavage cracks.

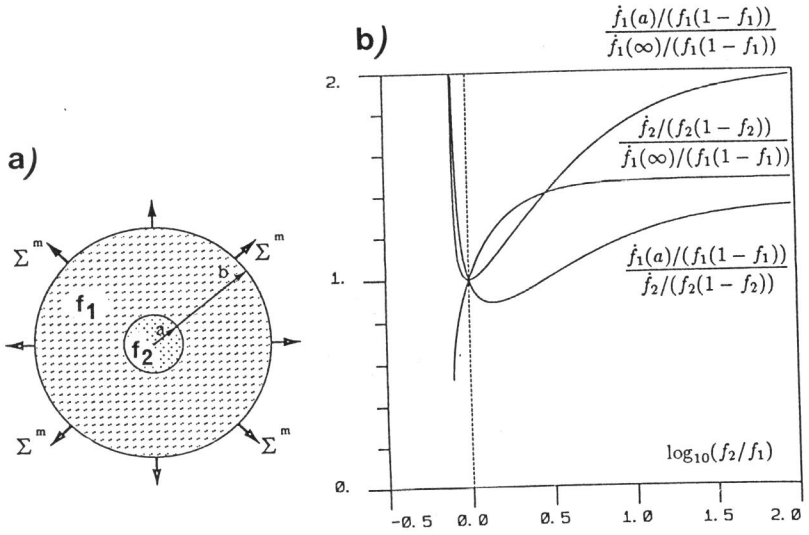

Figure 2 Model material with two populations of cavities. a) Model; b) Cavity growth as a function of f_2/f_1 ratio (Ref.[17]).

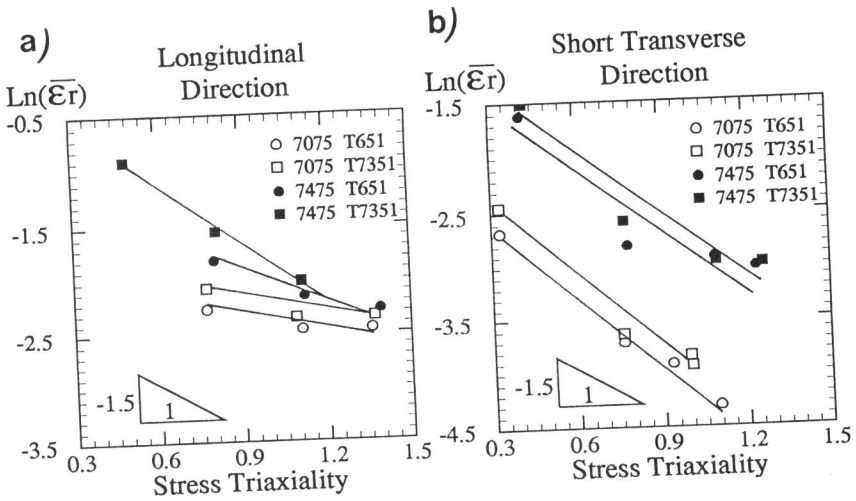

Figure 3 7075 and 7475Al Alloys. Ductility versus stress triaxiality. a) Longitudinal direction; b) Short transverse direction.

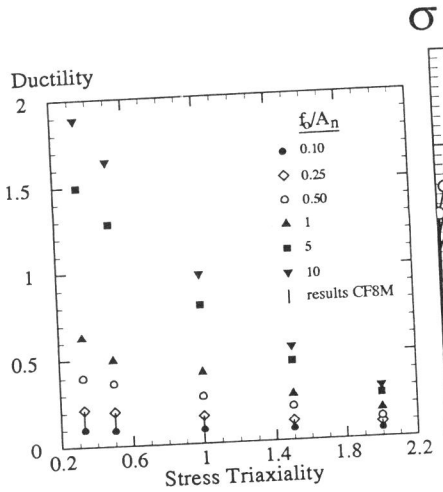

Figure 4 Ductility as a function of stress triaxiality for various values of the nucleation rate A_n.

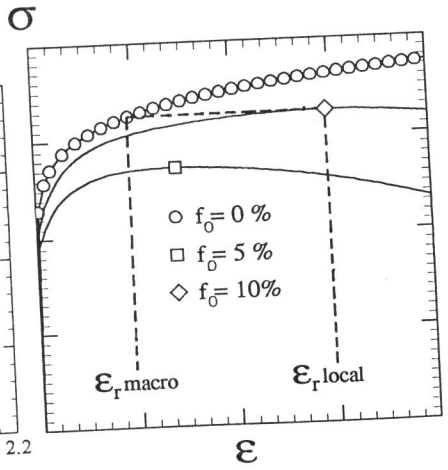

Figure 5 Softening effect due to the presence of cavities.

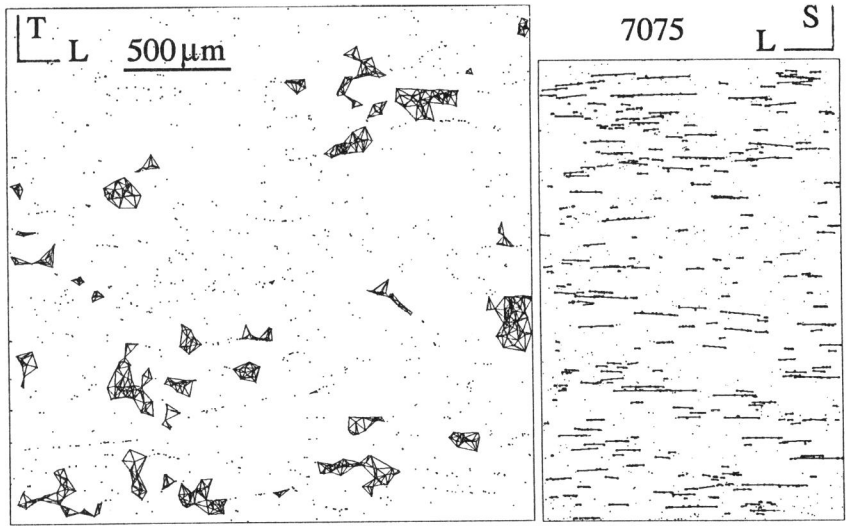

Figure 6 7075Al Alloy. Inclusion clusters determined by quantitative metallography in the a) TL plane; b) LS plane.

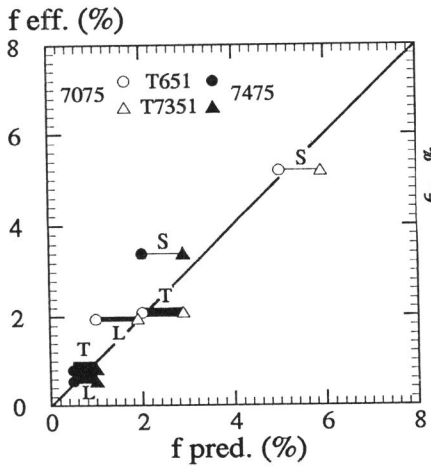

Figure 7 Comparison between the volume fraction of cavities at failure predicted (f_{pred}) and measured (f_{eff}) in 7075 and 7475 Alloys.

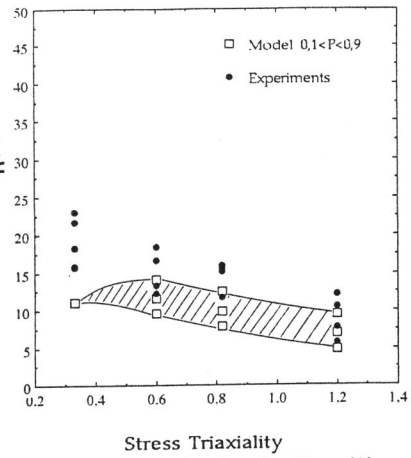

Figure 8 CF8M Steel. Ductility versus stress triaxiality. Comparison between calculated and experimental results.

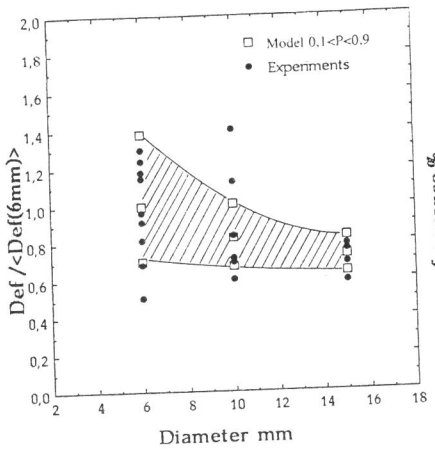

Figure 9 CF8M Steel. Effect of the size (minimum diameter) of notched specimens on the ductility.

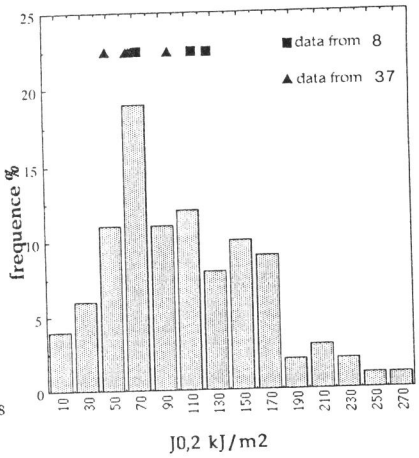

Figure 10 Distribution of $J_{0.2}$ results determined from the model. Comparison with some experimental results.

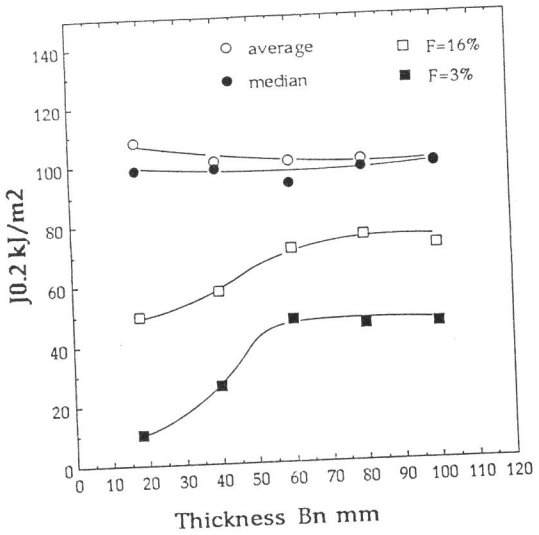

Figure 11 Effect of specimen width, B_n on the average, median , 16th and 3th percentile of $J_{0.2}$ as predicted by the model.